

CERN-EP-2019-173
8 August 2019

Global polarization of Λ and $\bar{\Lambda}$ hyperons in Pb–Pb collisions at the LHC

ALICE Collaboration*

Abstract

The global polarization of the Λ and $\bar{\Lambda}$ hyperons is measured for Pb–Pb collisions at $\sqrt{s_{NN}} = 2.76$ and 5.02 TeV recorded with the ALICE at the LHC. The results are reported differentially as a function of collision centrality and hyperon's transverse momentum (p_T) for the range of centrality 5–50%, $0.5 < p_T < 5$ GeV/ c , and rapidity $|y| < 0.5$. The hyperon global polarization averaged for Pb–Pb collisions at $\sqrt{s_{NN}} = 2.76$ and 5.02 TeV is found to be consistent with zero, $\langle P_H \rangle (\%) \approx 0.01 \pm 0.06$ (stat.) ± 0.03 (syst.) in the collision centrality range 15–50%, where the largest signal is expected. The results are compatible with expectations based on an extrapolation from measurements at lower collision energies at RHIC, hydrodynamical model calculations, and empirical estimates based on collision energy dependence of directed flow, all of which predict the global polarization values at LHC energies of the order of 0.01%.

arXiv:1909.01281v1 [nucl-ex] 3 Sep 2019

© 2019 CERN for the benefit of the ALICE Collaboration.

Reproduction of this article or parts of it is allowed as specified in the CC-BY-4.0 license.

*See Appendix A for the list of collaboration members

1 Introduction

The system created in a non-central nucleus–nucleus collision might retain a significant fraction of the large orbital angular momentum of the colliding nuclei. Due to the spin-orbit coupling, particles produced in such a collision can become globally polarized [1–4]. The measurements of a global polarization, when all particles are polarized along one preferential direction, provide important information about the initial conditions and dynamics of the quark-gluon plasma (QGP), as well as the hadronization process [5–7]. The global polarization for a specific particle and corresponding anti-particle is expected to be very similar, or even identical, in a system with small or zero baryon chemical potential.

High-energy heavy-ion collisions are also characterized by ultra-strong magnetic fields [8, 9], which on average are aligned with the direction of the angular momentum. While the peak values of the magnetic fields, which reach up to 10^{18} Gauss, can be estimated rather accurately [8, 9], the time evolution, which depends on the QGP electric conductivity, is practically unknown. These fields can also contribute to the global polarization, but their action on particles and anti-particles is expected to be in an opposite direction. Thus the measurement of the splitting between particle and anti-particle global polarizations provides very valuable information about the QGP properties.

The measurements of the global polarization P_H for spin one half Λ ($\bar{\Lambda}$) strange hyperons are experimentally favourable because their spin direction can be reconstructed via their weak decay topology into proton (anti-proton) and charged pion. Recently, the STAR Collaboration observed non-zero global polarization of Λ and $\bar{\Lambda}$ hyperons in Au–Au collisions, first for the RHIC beam energy scan (BES) energies of $\sqrt{s_{NN}} = 7 - 39$ GeV and, later, with more data, at $\sqrt{s_{NN}} = 200$ GeV [10, 11]. The magnitude of the observed polarization varies from a few to a fraction of a percent. While the P_H values for Λ and $\bar{\Lambda}$ agree within the experimental uncertainties, they are systematically higher for $\bar{\Lambda}$ than for Λ . Assuming that this difference originates due to the magnetic fields one estimates the field strength in units of elementary charge e to be $eB \sim 0.01m_\pi^2$ [12].

The exact nature of the spin-orbit interaction leading to the global polarization is not known. It is unclear at what stage of the system evolution (the QGP, hadronization, or the hadronic rescattering) the polarization is acquired, neither the corresponding relaxation times are known. Most of the recent calculations of the global polarization assume complete thermal equilibrium and validity of the hydrodynamical description of the system [6, 12–15]. They relate the particle polarization to the system’s thermal vorticity at the hadronization time. In a non-relativistic limit, assuming complete thermal equilibrium, the polarization of the particles can be evaluated as $\zeta = \langle \mathbf{s} \rangle / s = (s + 1) \boldsymbol{\omega} / (3T)$, where s is the particle’s spin, T is the system temperature, $\boldsymbol{\omega} = (1/2)(\nabla \times \mathbf{v})$ is a nonrelativistic vorticity, and \mathbf{v} is the local fluid velocity [12].

The global polarization is determined by the average vorticity component perpendicular to the collision reaction plane, which is spanned by the beam direction and the impact parameter vector. The global polarization measurements with the produced particle provide important information on both the nature of the spin-orbit interaction and the profile of velocity fields of the expanding system. Both, the magnitude and the direction of the vorticity, can strongly vary within the system [16]. In particular, a significant component along the beam direction can be acquired due to the transverse anisotropic flow [16, 17].

The vorticity of the system, especially its component along the system’s orbital momentum, is directly related to the asymmetries in the initial velocity fields. This links the vorticity with the directed flow v_1 , that is also strongly dependent on those asymmetries. The v_1 is defined by the first Fourier moment $v_1 = \langle \cos(\varphi - \Psi_{RP}) \rangle$ of the produced particle’s azimuthal asymmetry relative to the collision reaction plane angle Ψ_{RP} . Hydrodynamic simulations show that the orbital angular momentum stored in the system and the directed flow of charged particles are almost directly proportional to each other [5]. This allows for an empirical estimate of the collision energy dependence of the global polarization [16]. The STAR results for the directed flow [18, 19] and the hyperon global polarization [10, 11] from the BES program show that the slopes of v_1 at midrapidity ($dv_1/d\eta$) for charged hadrons (pions) and the hyperon

polarization are indeed strongly correlated. The charged-particle directed flow in Pb–Pb collisions at $\sqrt{s_{\text{NN}}} = 2.76$ TeV is about three times smaller [20] than at the top RHIC energy of 200 GeV. This suggests that the global polarization at the LHC energies should be also about three times smaller than at RHIC (around $\sim 0.08\%$) and decreasing from $\sqrt{s_{\text{NN}}} = 2.76$ TeV to 5.02 TeV by about $\sim 30\%$ [21]. Even smaller polarization values at the LHC are expected when the directed flow is seen as a combination of the two effects – the tilt of the source in the longitudinal direction and the dipole flow originating from the asymmetry in the initial energy density distributions [22]. Taking into account that only the contribution to the directed flow from the tilted source is related to the vorticity and that its contribution relative to the dipole flow decreases with the collision energy [22], one arrives to an estimate for the global polarization at the LHC energies of the order of $\sim 0.04\%$.

In this paper, the measurements of the global polarization of the Λ and $\bar{\Lambda}$ hyperons in Pb–Pb collisions at $\sqrt{s_{\text{NN}}} = 2.76$ and 5.02 TeV recorded with ALICE at the LHC are reported. The paper is organized as follows. In Sec. 2 the analysis details are presented, and the global polarization observable is introduced, as well as the measurement technique. The various sources of systematic uncertainties are discussed in Sec. 3. The results for the Λ and $\bar{\Lambda}$ global polarization at two collision energies as a function of the hyperon transverse momentum and collision centrality are presented in Sec. 4.

2 Data analysis

2.1 The observable

In this measurement, Λ and $\bar{\Lambda}$ hyperons are reconstructed through their weak decay topologies $\Lambda \rightarrow p + \pi^-$ and $\bar{\Lambda} \rightarrow \bar{p} + \pi^+$ (64% branching ratio). The global polarization of the hyperons is determined from the angular distributions of their decay (anti-)protons. In the hyperon rest frame, the (anti-)proton angular probability distribution, $dw/d\mathbf{n}_p^*$, is given by

$$\frac{dw}{d\mathbf{n}_p^*} = 1 + \alpha_H \boldsymbol{\zeta}_H \cdot \mathbf{n}_p^*, \quad (1)$$

where \mathbf{n}_p^* is the unit vector of the (anti-)proton direction. The $\alpha_H = \pm(0.642 \pm 0.013)$, positive for Λ and negative for $\bar{\Lambda}$, is the hyperon decay parameter [23]. The same absolute value of α_H is used for Λ and $\bar{\Lambda}$. The polarization vector $\boldsymbol{\zeta}_H$ in Eq. (1), which is satisfying condition $|\boldsymbol{\zeta}_H| \leq 1$, can be measured experimentally as [24]

$$\boldsymbol{\zeta}_H = \frac{3}{\alpha_H} \langle \mathbf{n}_p^* \rangle, \quad (2)$$

where the brackets $\langle \dots \rangle$ denote an event-by-event averaging over all hyperon decays.

The polarization vector $\boldsymbol{\zeta}_H$ generally depends on the hyperon kinematics, namely the transverse momentum p_T , rapidity y , and its azimuthal angle with respect to the reaction plane, $\varphi - \Psi_{\text{RP}}$, as well as the collision centrality. The global polarization reported in this paper is determined by the component of the polarization vector perpendicular to the reaction plane. The magnitude P_H of the global polarization can be measured by averaging a corresponding projection of the \mathbf{n}_p^* vector, which in the laboratory coordinate system is given by $n_{p\perp\text{RP}}^* = \sin \theta_p^* \sin(\varphi_p^* - \Psi_{\text{RP}})$. Here θ_p^* (φ_p^*) is the polar angle with respect to the collision axis (azimuthal angle) of the (anti-)proton direction in the hyperon rest frame. Substituting $n_{p\perp\text{RP}}^*$ into Eq. (2) and assuming an ideal detector acceptance, an average over the θ_p^* yields

$$P_H = \frac{8}{\pi \alpha_H} \langle \sin(\varphi_p^* - \Psi_{\text{RP}}) \rangle. \quad (3)$$

Here the brackets $\langle \dots \rangle$ imply averaging over individual hyperons in all events. The polarization is defined to be positive if the hyperon spin has a positive component along the system's angular momentum –

the same convention as employed in [10]. The detector acceptance effects are treated in this work as systematic uncertainty and discussed in Sec. 3.

A significant fraction of Λ and $\bar{\Lambda}$ hyperons originates from decay of heavier particles. Existing estimates [6, 12, 13] of the feed-down effect on the hyperon global polarization measurements, based on the assumption of thermal equilibrium and the particle yields from the statistical model [25], suggest that the primary Λ and $\bar{\Lambda}$ polarization should be by about 15–20% larger than what is measured at RHIC. Taking into account that feed-down effects are expected to be small compared to other uncertainties in the current analysis, no correction to the data have been applied.

2.2 Measurement technique

The main components of the ALICE detector system [26, 27] used for this measurement are the Time Projection Chamber (TPC) [28], the silicon detectors of the Inner Tracking System (ITS) [29] and the two neutron Zero-Degree Calorimeters (ZDC) [30]. The analyzed data samples were recorded by ALICE in 2010 and 2011 for Pb–Pb collisions at $\sqrt{s_{\text{NN}}} = 2.76$ TeV, and in 2015 for collisions at $\sqrt{s_{\text{NN}}} = 5.02$ TeV.

During the data taking, the trigger required a hit in a pair of V0 detectors [31]. In 2010 and 2011, events with only one V0 hit and at least two hits in the outer layer of the Silicon Pixel Detector (SPD) were accepted as well. Contamination from beam-induced background was removed offline, as discussed in [32, 33]. The events with poor correlation between multiplicities in V0, ITS and TPC detectors were rejected. The analysis was restricted to the events with the primary vertex along the beam direction, V_z , within ± 10 cm from the nominal center of the TPC. This yielded for all collision centralities approximately 49 (75) million of Pb–Pb collisions at $\sqrt{s_{\text{NN}}} = 2.76$ (5.02) TeV. The collision centrality was determined using the energy deposition in the V0 detectors [34].

The reaction plane angle Ψ_{RP} was estimated using the spectator plane angle Ψ_{SP} , characterizing the deflection direction of the spectator neutrons. The spectator deflections at positive and negative rapidity were reconstructed with a pair of neutron ZDC detectors located 114 m away from the interaction point. The Ψ_{SP} angle was evaluated separately for the two detectors using the transverse profile of the spectator energy distribution provided by the 2×2 segmentation of the ZDCs. For this, a pair of two-dimensional vectors $\mathbf{Q}^{\text{t,p}}$ were constructed for two ZDCs following the procedure described in [20]:

$$\mathbf{Q}^{\text{t,p}} \equiv (Q_x^{\text{t,p}}, Q_y^{\text{t,p}}) = \sum_{i=1}^4 \mathbf{n}_i E_i^{\text{t,p}} / \sum_{i=1}^4 E_i^{\text{t,p}}, \quad (4)$$

where p (t) denotes the ZDC on the projectile, $\eta > 0$ (target, $\eta < 0$) side of the interaction point, E_i is the measured signal and $\mathbf{n}_i = (x_i, y_i)$ are the coordinates of the i -th ZDC segment. The event averaged $\langle \mathbf{Q}^{\text{t,p}} \rangle$ revealed a strong dependence on the collision centrality as well as on the three collision vertex coordinates, which is imposed by the offset of the LHC beam transverse spot positions relative to the nominal center of the ZDCs. Moreover, the $\langle \mathbf{Q}^{\text{t,p}} \rangle$ demonstrated a strong time dependence in some of the 2015 runs. To compensate for these variations an event-by-event re-centering correction [35] was applied as a function of collision centrality, three components of the collision vertex position, and beam time variation

$$\mathbf{Q}' = \mathbf{Q} - \langle \mathbf{Q} \rangle. \quad (5)$$

Additionally to the procedure described in [20], the width of the \mathbf{Q}' distributions was equalized as a function of centrality, which together with Eq. (5) resulted in an overall \mathbf{Q} -vector correction

$$Q_x'' = \frac{Q_x' - \langle Q_x \rangle}{\langle Q_x^2 \rangle}, \quad Q_y'' = \frac{Q_y' - \langle Q_y \rangle}{\langle Q_y^2 \rangle}. \quad (6)$$

The width equalization, up to 20%, turned out to be particularly useful for the 2015 data sample, where one of the two neutron ZDC detectors lost signal from one of its four channels.

The Ψ_{SP} angle estimated from each ZDC is then given by the direction of the corrected \mathbf{Q}'' vector

$$\mathbf{Q}'' = |\mathbf{Q}''| \exp\{i\Psi_{\text{SP}}\}. \quad (7)$$

To account for a finite resolution of the spectator plane angle Ψ_{SP} , a correction $R_{\text{SP}}^{(1)}$ is introduced in the Eq. (3) following the method described in [24]

$$P_{\text{H}} = \frac{8}{\pi\alpha_{\text{H}}} \frac{\langle \sin(\varphi_{\text{p}}^* - \Psi_{\text{SP}}) \rangle}{R_{\text{SP}}^{(1)}}. \quad (8)$$

The polarization values obtained with Eq. (8) for each of the two ZDC detectors were found to be similar within the statistical uncertainties and were combined.

The correction $R_{\text{SP}}^{(1)}$ was extracted from correlations between \mathbf{Q} -vector angles from different ALICE detectors following the technique described in [36]. Figure 1 presents the $R_{\text{SP}}^{(1)}$ as a function of collision centrality for different data sets. The most central (0–5%) collisions are excluded from the analysis,

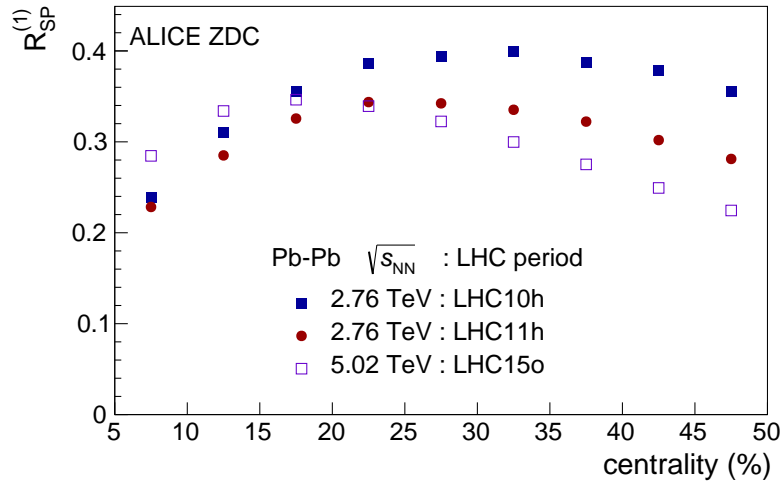


Fig. 1: (color online) The correction $R_{\text{SP}}^{(1)}$ for finite resolution of the spectator plane angle Ψ_{SP} as a function of collision centrality for three data sets used in the analysis. Only statistical uncertainties, which are smaller than a symbol size, are shown.

because the small number of spectators does not allow for reliable estimation of the spectator deflection with the ZDCs. During the Pb–Pb data taking in 2011 ($\sqrt{s_{\text{NN}}} = 2.76$ TeV) and 2015 ($\sqrt{s_{\text{NN}}} = 5.02$ TeV), the beams were collided at a non-zero vertical crossing angle [27]. This resulted in a partial screening of the spectator neutrons by the LHC tertiary collimators [37] and in a degradation of the spectator plane resolution. The V0s, TPC, and two forward multiplicity detectors (FMD) [38] were used to estimate a possible uncertainties in $R_{\text{SP}}^{(1)}$ extraction for the two ZDC detectors. In all data samples, these uncertainties turned out to be at a level of several percent.

The Λ and $\bar{\Lambda}$ hyperons were reconstructed via their weak decay topology following the method and selection criteria described in [27, 39]. Charged daughter tracks from hyperon decay were required to have the pseudo-rapidity $|\eta| < 0.9$ and at least 70 space points in the TPC. The pion and (anti-)proton particle type assignments were based on the track charge and specific energy loss (dE/dx) measured in the TPC. The daughter tracks were paired to form Λ and $\bar{\Lambda}$ candidates. The candidates were required to have transverse momentum $p_{\text{T}} > 0.5$ GeV/ c , rapidity $|y| < 0.5$, and the momentum vector pointing back to the primary collision vertex within a cone of opening angle less than 0.1 (0.08) radians for Pb–Pb collisions at $\sqrt{s_{\text{NN}}} = 2.76$ (5.02) TeV.

The hyperon global polarization P_H was extracted with the fit to the measured correlation $\langle \sin(\phi_p^* - \Psi_{SP}) \rangle$ as a function of the Λ or $\bar{\Lambda}$ candidate invariant mass, M_{inv} :

$$\langle \sin(\phi_p^* - \Psi_{SP}) \rangle (M_{\text{inv}}) = [1 - f_{\text{BG}}(M_{\text{inv}})] \times S_H + f_{\text{BG}}(M_{\text{inv}}) \times L_{\text{BG}}(M_{\text{inv}}). \quad (9)$$

Here the constant S_H gives the numerator of Eq. (8) and $L(M_{\text{inv}})$ is a linear parameterization of the background correlation as a function of M_{inv} . The background fraction $f_{\text{BG}}(M_{\text{inv}})$ was evaluated as

$$f_{\text{BG}}(M_{\text{inv}}) = \frac{N_{\text{BG}}(M_{\text{inv}})}{N_{\text{tot}}(M_{\text{inv}})}. \quad (10)$$

Here $N_{\text{tot}}(M_{\text{inv}})$ is the total measured yield of the Λ or $\bar{\Lambda}$ candidates. The $N_{\text{BG}}(M_{\text{inv}})$ is given by the 4-th order polynomial fit to the $N_{\text{tot}}(M_{\text{inv}})$ outside of the Λ and $\bar{\Lambda}$ invariant mass peak range, $M_{\text{inv}} < 1.107 \text{ GeV}/c^2$ and $M_{\text{inv}} > 1.125 \text{ GeV}/c^2$.

The fitting procedure is illustrated in Fig. 2 for 20–30% centrality range in Pb–Pb collisions at $\sqrt{s_{\text{NN}}} = 2.76 \text{ TeV}$ using data collected during the LHC operation in 2011.

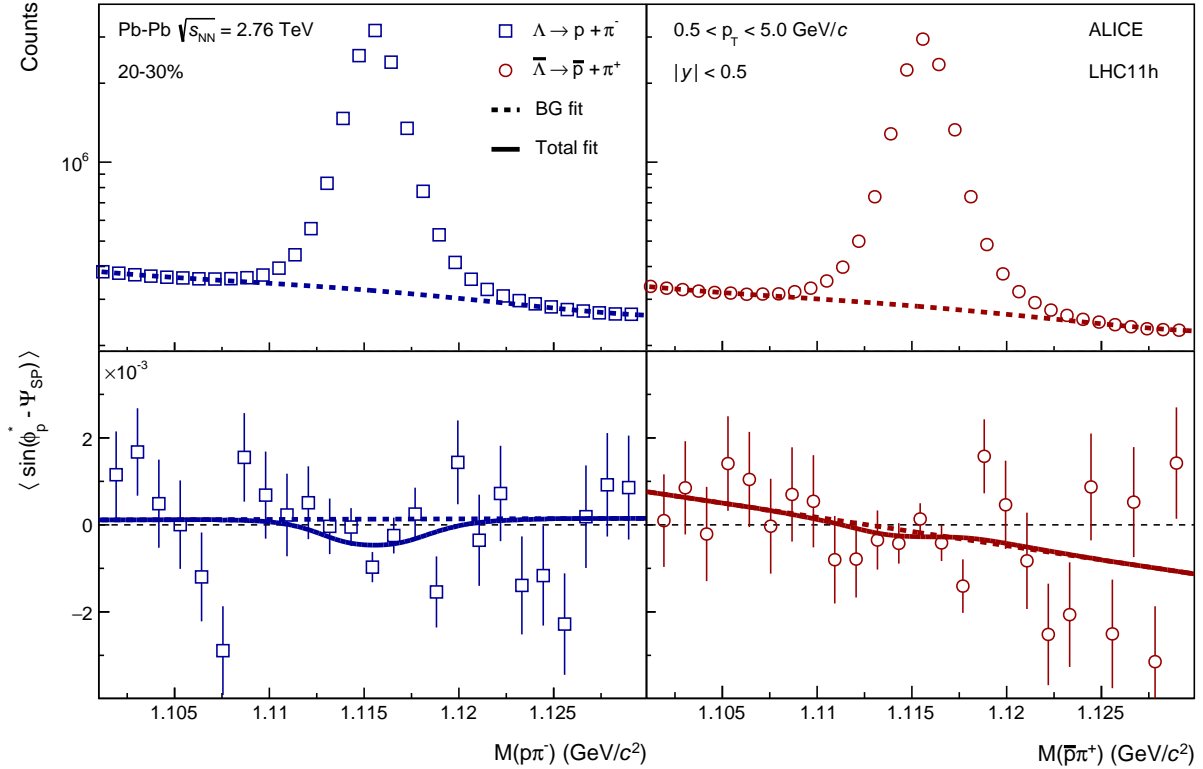


Fig. 2: (color online) (Upper panels) invariant mass distributions of Λ (left) and $\bar{\Lambda}$ (right) candidates for 20–30% centrality range in Pb–Pb collisions at $\sqrt{s_{\text{NN}}} = 2.76 \text{ TeV}$ using data collected during the LHC operation in 2011. Dashed lines show the result of the fit for $N_{\text{BG}}(M_{\text{inv}})$ in Eq. (10). (Bottom panels) Global polarization extraction via fit to $\langle \sin(\phi_p^* - \Psi_{SP}) \rangle$ as a function of the invariant mass, with Ψ_{SP} reconstructed with the ZDC on the target ($\eta < 0$) side. Dashed and solid lines show $L_{\text{BG}}(M_{\text{inv}})$ and the combined fit with Eq. (9). See text for more details.

3 Systematic uncertainties

The considered sources of systematic uncertainties are summarized in Table 1. The significance of a given systematical variation is determined following the procedure presented in [40].

The selection on the primary vertex position V_z was varied to $\pm 7 \text{ cm}$ and $\pm 8 \text{ cm}$ instead of the default $\pm 10 \text{ cm}$. The analysis was repeated with the collision centrality estimated with either ITS or TPC

Table 1: Systematic uncertainties in global polarization measurements for different data sets. Values reported as a fraction of the corresponding statistical uncertainty.

Data sample	centrality	$\Lambda/\bar{\Lambda}$ candidate selection	Fitting procedure	Acceptance	$R_{SP}^{(1)}$
2010	5–15% 15–50%	20%	30% 5%	10%	< 2%
2011	5–15% 15–50%	30%	20% 12%	10%	< 2%
2015	5–50%	30%	20%	10%	< 4%

detectors (instead of default V0 detector). Variations of the results when changing the event selection criteria described above and centrality estimators are found to be negligible and were not included into the total systematic uncertainty.

The following Λ and $\bar{\Lambda}$ candidate selection criteria were varied: the distance of closest approach to the primary vertex, decay daughter track selection via specific energy loss in the TPC, the distance of closest approach between the pair of the daughter tracks, and the criteria on the hyperon candidates momentum pointing angle to the primary vertex. The corresponding contribution from these variations to the total systematic uncertainty is about 20–30% of the statistical uncertainty. The main contribution to the systematic uncertainty from the fitting procedure in Eq. (9) comes from a variation of the fit region.

In Eq. (8) a perfect acceptance of the hyperons and their decay daughters is assumed. In the case of an imperfect detector, there is a overall scale correction of the measured polarization as well as a possible admixture of higher-order harmonics in a Fourier decomposition of the $dN_{\Lambda/\bar{\Lambda}}/d(\varphi_p^* - \Psi_{RP})$ distribution. Using the method described in [24, 41] the corresponding relative uncertainty was estimated to be about 10% independent of centrality. This uncertainty comes primarily from the admixture of the higher-order harmonics when hyperon $p_T \lesssim 2$ GeV/c.

A detailed study was performed for the evaluation of the systematic uncertainties of $R_{SP}^{(1)}$ as well as for the evaluation of the difference between the two neutron ZDC detectors. The correlations between the flow vectors from different detectors, including TPC and pairs of ZDC, V0, FMD detectors were studied. The contribution the total systematic uncertainties due to the $R_{SP}^{(1)}$ extraction were found to be at a level of a few percent.

4 Results

Figures 3 and 4 show the measured hyperon global polarization P_H as a function of centrality and hyperon transverse momentum, p_T , in Pb–Pb collisions for two collision energies. The results from 2010 and 2011 data samples were combined accounting for the corresponding statistical and systematic uncertainty. At RHIC energies, the global polarization exhibited a clear centrality dependence with three times large magnitude in peripheral collisions compared to that in central, while no significant p_T dependence within the accessible p_T range was observed [11]. The P_H at the LHC is found to be consistent with zero within the experimental uncertainties for all studied centrality classes (Fig. 3) and p_T ranges (Fig. 4). By repeating a similar analysis, no signal signal was observed as a function of rapidity either.

The average global polarization for two centrality ranges, 5–15% and 15–50%, are presented in Fig. 5, while numerical values are reported in Tab. 2. Figure 5 also presents the comparison with the STAR data [10, 11] for lower collision energies. Despite large uncertainties, the ALICE measurements confirm the trend of the global polarization decreasing with increasing collision energy.

Assuming the same values of the global polarization for Λ and $\bar{\Lambda}$ and neglecting the possible difference of about 30% (according to the empirical estimates discussed above) between the two LHC energies, one

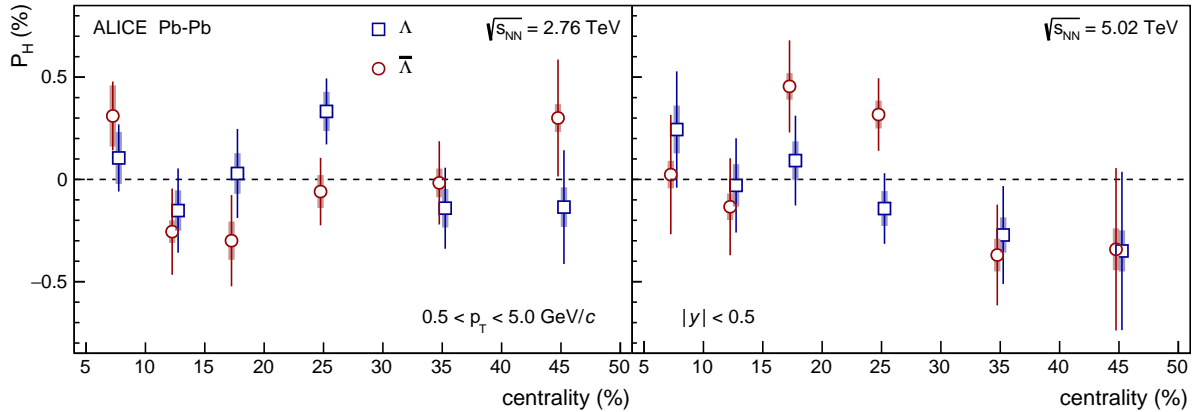


Fig. 3: (color online) The global hyperon polarization as function of centrality for Pb–Pb collisions at $\sqrt{s_{\text{NN}}} = 2.76$ TeV (left) and 5.02 TeV (right). The systematic uncertainties are shown as shaded boxes. Points are slightly shifted along the horizontal axis for better visibility.

can average all four ALICE data points for 15–50% centrality, where the largest signal is expected. This yields a value $\langle P_H \rangle (\%) \approx 0.01 \pm 0.06$ (stat.) ± 0.03 (syst.) for 15–50% centrality, which is consistent with the empirical estimates of $P_H(\%) \approx 0.04 - 0.08$ based on directed flow measurements.

Table 2: The global polarization of Λ and $\bar{\Lambda}$ hyperons in Pb–Pb collisions at $\sqrt{s_{\text{NN}}} = 2.76$ TeV and 5.02 TeV for centrality ranges 5–15% and 15–50%.

$\sqrt{s_{\text{NN}}}$	centrality	$P_{\Lambda}(\%)$	$P_{\bar{\Lambda}}(\%)$
2.76 TeV	5–15%	0.01 ± 0.13 (stat.) ± 0.04 (syst.)	0.09 ± 0.13 (stat.) ± 0.08 (syst.)
	15–50%	0.08 ± 0.10 (stat.) ± 0.04 (syst.)	-0.05 ± 0.10 (stat.) ± 0.03 (syst.)
5.02 TeV	5–15%	0.08 ± 0.18 (stat.) ± 0.08 (syst.)	-0.07 ± 0.18 (stat.) ± 0.03 (syst.)
	15–50%	-0.13 ± 0.11 (stat.) ± 0.04 (syst.)	0.14 ± 0.12 (stat.) ± 0.03 (syst.)
average	15–50%	$\langle P_H \rangle (\%) \approx 0.01 \pm 0.06$ (stat.) ± 0.03 (syst.)	

5 Summary

The first measurements of Λ and $\bar{\Lambda}$ hyperons global polarization are reported for Pb–Pb collisions at $\sqrt{s_{\text{NN}}} = 2.76$ and 5.02 TeV recorded with ALICE at the LHC. The hyperon global polarization has been measured differentially as a function of centrality and transverse momentum (p_T) for the range of collision centrality 5–50%, $0.5 < p_T < 5$ GeV/ c , and rapidity $|y| < 0.5$. No significant dependences neither splitting between the global polarization values for Λ and $\bar{\Lambda}$ has been observed. The average Λ and $\bar{\Lambda}$ polarization for 15–50% centrality range at two collision energies is $\langle P_H \rangle (\%) \approx 0.01 \pm 0.06$ (stat.) ± 0.03 (syst.). This confirms the observed earlier trend of the global polarization decrease with increasing collision energy. The results are compatible with the extrapolation of the RHIC results and empirical estimates of $P_H(\%) \approx 0.04 - 0.08$ based on the similarity of collision energy dependence of the global polarization and the slope of the directed flow in the midrapidity region. The high luminosity LHC run after the 2019–2021 long shutdown with the upgraded ALICE detector will bring more than 100 times more data, which should allow tests of the previously mentioned prediction with much better accuracy.

Acknowledgements

The ALICE Collaboration would like to thank all its engineers and technicians for their invaluable contributions to the construction of the experiment and the CERN accelerator teams for the outstanding performance of the LHC complex. The ALICE Collaboration gratefully acknowledges the resources and

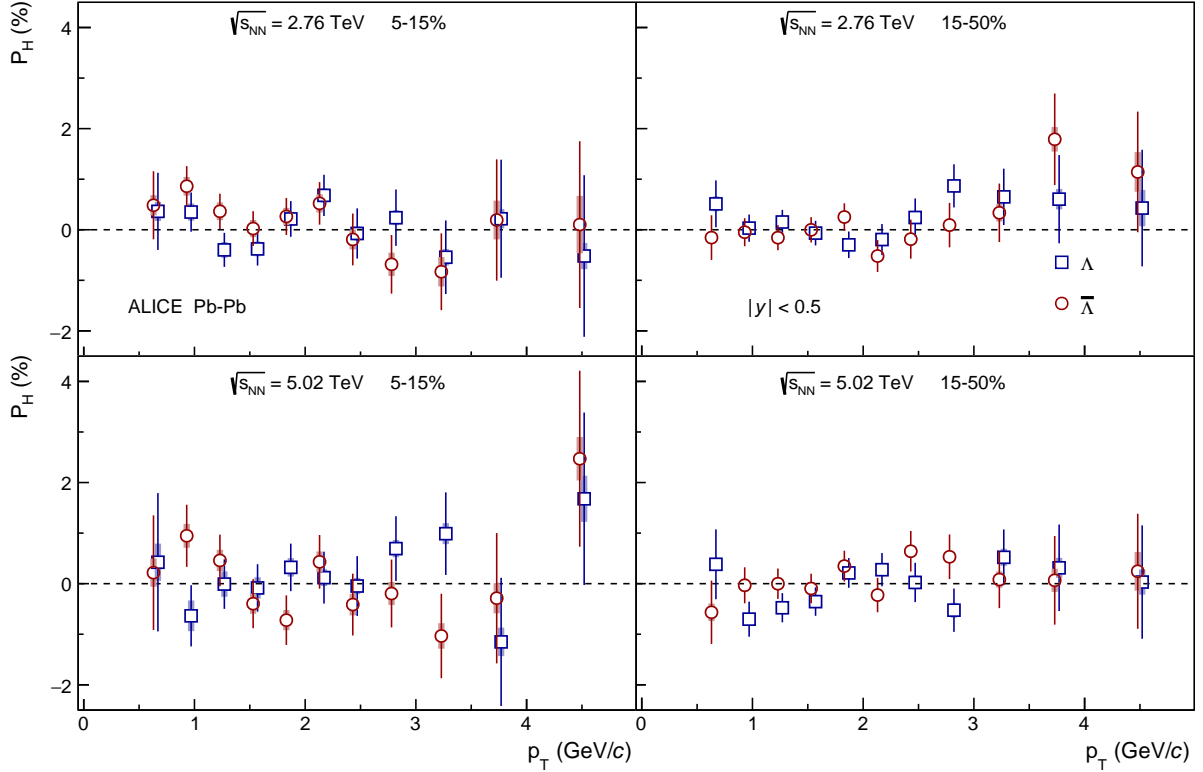


Fig. 4: (color online) The global hyperon polarization as function of transverse momentum p_T for Pb–Pb collisions at $\sqrt{s_{NN}} = 2.76$ TeV (upper) and 5.02 TeV (lower) in 5–15% (left) and 15–50% (right) centrality classes. The systematic uncertainties are shown as shaded boxes. Points are slightly shifted along the horizontal axis for better visibility.

support provided by all Grid centres and the Worldwide LHC Computing Grid (WLCG) collaboration. The ALICE Collaboration acknowledges the following funding agencies for their support in building and running the ALICE detector: A. I. Alikhanyan National Science Laboratory (Yerevan Physics Institute) Foundation (ANSL), State Committee of Science and World Federation of Scientists (WFS), Armenia; Austrian Academy of Sciences, Austrian Science Fund (FWF): [M 2467-N36] and Nationalstiftung für Forschung, Technologie und Entwicklung, Austria; Ministry of Communications and High Technologies, National Nuclear Research Center, Azerbaijan; Conselho Nacional de Desenvolvimento Científico e Tecnológico (CNPq), Financiadora de Estudos e Projetos (Finep), Fundação de Amparo à Pesquisa do Estado de São Paulo (FAPESP) and Universidade Federal do Rio Grande do Sul (UFRGS), Brazil; Ministry of Education of China (MOEC), Ministry of Science & Technology of China (MSTC) and National Natural Science Foundation of China (NSFC), China; Ministry of Science and Education and Croatian Science Foundation, Croatia; Centro de Aplicaciones Tecnológicas y Desarrollo Nuclear (CEADEN), Cubaenergía, Cuba; Ministry of Education, Youth and Sports of the Czech Republic, Czech Republic; The Danish Council for Independent Research | Natural Sciences, the VILLUM FONDEN and Danish National Research Foundation (DNRF), Denmark; Helsinki Institute of Physics (HIP), Finland; Commissariat à l’Energie Atomique (CEA), Institut National de Physique Nucléaire et de Physique des Particules (IN2P3) and Centre National de la Recherche Scientifique (CNRS) and Région des Pays de la Loire, France; Bundesministerium für Bildung und Forschung (BMBF) and GSI Helmholtzzentrum für Schwerionenforschung GmbH, Germany; General Secretariat for Research and Technology, Ministry of Education, Research and Religions, Greece; National Research, Development and Innovation Office, Hungary; Department of Atomic Energy Government of India (DAE), Department of Science and Technology, Government of India (DST), University Grants Commission, Government of India (UGC) and Council of Scientific and Industrial Research (CSIR), India; Indonesian Institute of Science, Indonesia;

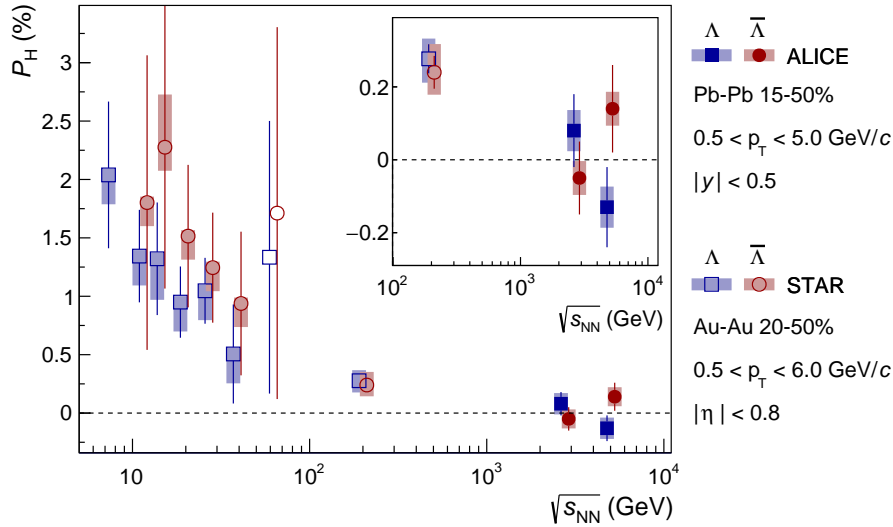


Fig. 5: (color online) The global hyperon polarization as a function of collision energy. Results are compared with the STAR data at lower energies [10, 11]. The insert shows zoomed-in comparison with the data at the top RHIC energy. The systematic uncertainties are shown as shaded boxes. Points are slightly shifted along the horizontal axis for better visibility.

Centro Fermi - Museo Storico della Fisica e Centro Studi e Ricerche Enrico Fermi and Istituto Nazionale di Fisica Nucleare (INFN), Italy; Institute for Innovative Science and Technology, Nagasaki Institute of Applied Science (IIST), Japanese Ministry of Education, Culture, Sports, Science and Technology (MEXT) and Japan Society for the Promotion of Science (JSPS) KAKENHI, Japan; Consejo Nacional de Ciencia (CONACYT) y Tecnología, through Fondo de Cooperación Internacional en Ciencia y Tecnología (FONCICYT) and Dirección General de Asuntos del Personal Académico (DGAPA), Mexico; Nederlandse Organisatie voor Wetenschappelijk Onderzoek (NWO), Netherlands; The Research Council of Norway, Norway; Commission on Science and Technology for Sustainable Development in the South (COMSATS), Pakistan; Pontificia Universidad Católica del Perú, Peru; Ministry of Science and Higher Education and National Science Centre, Poland; Korea Institute of Science and Technology Information and National Research Foundation of Korea (NRF), Republic of Korea; Ministry of Education and Scientific Research, Institute of Atomic Physics and Ministry of Research and Innovation and Institute of Atomic Physics, Romania; Joint Institute for Nuclear Research (JINR), Ministry of Education and Science of the Russian Federation, National Research Centre Kurchatov Institute, Russian Science Foundation and Russian Foundation for Basic Research, Russia; Ministry of Education, Science, Research and Sport of the Slovak Republic, Slovakia; National Research Foundation of South Africa, South Africa; Swedish Research Council (VR) and Knut & Alice Wallenberg Foundation (KAW), Sweden; European Organization for Nuclear Research, Switzerland; Suranaree University of Technology (SUT), National Science and Technology Development Agency (NSDTA) and Office of the Higher Education Commission under NRU project of Thailand, Thailand; Turkish Atomic Energy Agency (TAEK), Turkey; National Academy of Sciences of Ukraine, Ukraine; Science and Technology Facilities Council (STFC), United Kingdom; National Science Foundation of the United States of America (NSF) and United States Department of Energy, Office of Nuclear Physics (DOE NP), United States of America.

References

- [1] Z.-T. Liang and X.-N. Wang, “Globally polarized quark-gluon plasma in non-central A+A collisions,” *Phys. Rev. Lett.* **94** (2005) 102301, arXiv:nucl-th/0410079 [nucl-th]. [Erratum: *Phys. Rev. Lett.* 96,039901(2006)].

- [2] S. A. Voloshin, “Polarized secondary particles in unpolarized high energy hadron-hadron collisions?,” arXiv:nucl-th/0410089 [nucl-th].
- [3] Z.-T. Liang and X.-N. Wang, “Spin alignment of vector mesons in non-central A+A collisions,” *Phys. Lett.* **B629** (2005) 20–26, arXiv:nucl-th/0411101 [nucl-th].
- [4] J.-H. Gao, S.-W. Chen, W.-t. Deng, Z.-T. Liang, Q. Wang, and X.-N. Wang, “Global quark polarization in non-central A+A collisions,” *Phys. Rev.* **C77** (2008) 044902, arXiv:0710.2943 [nucl-th].
- [5] F. Becattini, G. Inghirami, V. Rolando, A. Beraudo, L. Del Zanna, A. De Pace, M. Nardi, G. Pagliara, and V. Chandra, “A study of vorticity formation in high energy nuclear collisions,” *Eur. Phys. J.* **C75** no. 9, (2015) 406, arXiv:1501.04468 [nucl-th]. [Erratum: *Eur. Phys. J.* **C78**,no.5,354(2018)].
- [6] H. Li, L.-G. Pang, Q. Wang, and X.-L. Xia, “Global Λ polarization in heavy-ion collisions from a transport model,” *Phys. Rev.* **C96** no. 5, (2017) 054908, arXiv:1704.01507 [nucl-th].
- [7] Y. Xie, D. Wang, and L. P. Csernai, “Global Λ polarization in high energy collisions,” *Phys. Rev.* **C95** no. 3, (2017) 031901, arXiv:1703.03770 [nucl-th].
- [8] V. Skokov, A. Yu. Illarionov, and V. Toneev, “Estimate of the magnetic field strength in heavy-ion collisions,” *Int. J. Mod. Phys.* **A24** (2009) 5925–5932, arXiv:0907.1396 [nucl-th].
- [9] K. Tuchin, “Particle production in strong electromagnetic fields in relativistic heavy-ion collisions,” *Adv. High Energy Phys.* **2013** (2013) 490495, arXiv:1301.0099 [hep-ph].
- [10] **STAR** Collaboration, L. Adamczyk *et al.*, “Global Λ hyperon polarization in nuclear collisions: evidence for the most vortical fluid,” *Nature* **548** (2017) 62–65, arXiv:1701.06657 [nucl-ex].
- [11] **STAR** Collaboration, J. Adam *et al.*, “Global polarization of Λ hyperons in Au+Au collisions at $\sqrt{s_{NN}} = 200$ GeV,” *Phys. Rev.* **C98** (2018) 014910, arXiv:1805.04400 [nucl-ex].
- [12] F. Becattini, I. Karpenko, M. Lisa, I. Upszal, and S. Voloshin, “Global hyperon polarization at local thermodynamic equilibrium with vorticity, magnetic field and feed-down,” *Phys. Rev.* **C95** no. 5, (2017) 054902, arXiv:1610.02506 [nucl-th].
- [13] I. Karpenko and F. Becattini, “Study of Λ polarization in relativistic nuclear collisions at $\sqrt{s_{NN}} = 7.7$ – 200 GeV,” *Eur. Phys. J.* **C77** no. 4, (2017) 213, arXiv:1610.04717 [nucl-th].
- [14] W. Florkowski, B. Friman, A. Jaiswal, and E. Speranza, “Relativistic fluid dynamics with spin,” *Phys. Rev.* **C97** no. 4, (2018) 041901, arXiv:1705.00587 [nucl-th].
- [15] M. Baznat, K. Gudima, A. Sorin, and O. Teryaev, “Hyperon polarization in heavy-ion collisions and holographic gravitational anomaly,” *Phys. Rev.* **C97** no. 4, (2018) 041902, arXiv:1701.00923 [nucl-th].
- [16] S. A. Voloshin, “Vorticity and particle polarization in heavy ion collisions (experimental perspective),” arXiv:1710.08934 [nucl-ex]. [EPJ Web Conf.17,10700(2018)].
- [17] F. Becattini and I. Karpenko, “Collective Longitudinal Polarization in Relativistic Heavy-Ion Collisions at Very High Energy,” *Phys. Rev. Lett.* **120** no. 1, (2018) 012302, arXiv:1707.07984 [nucl-th].
- [18] **STAR** Collaboration, L. Adamczyk *et al.*, “Beam-Energy Dependence of the Directed Flow of Protons, Antiprotons, and Pions in Au+Au Collisions,” *Phys. Rev. Lett.* **112** no. 16, (2014) 162301, arXiv:1401.3043 [nucl-ex].

- [19] **STAR** Collaboration, P. Shanmuganathan, “Beam-Energy and Centrality Dependence of Directed Flow of Identified Particles,” *Nucl. Phys.* **A956** (2016) 260–263, arXiv:1512.09009 [nucl-ex].
- [20] **ALICE** Collaboration, B. Abelev *et al.*, “Directed Flow of Charged Particles at Midrapidity Relative to the Spectator Plane in Pb-Pb Collisions at $\sqrt{s_{NN}}=2.76$ TeV,” *Phys. Rev. Lett.* **111** no. 23, (2013) 232302, arXiv:1306.4145 [nucl-ex].
- [21] **ALICE** Collaboration, J. Margutti, “The search for magnetic-induced charged currents in Pb–Pb collisions with ALICE,” in *12th Workshop on Particle Correlations and Femtoscopy (WPCF 2017) Amsterdam, Netherlands, June 12-16, 2017*. 2017. arXiv:1709.05618 [nucl-ex].
- [22] **STAR** Collaboration, L. Adamczyk *et al.*, “Azimuthal anisotropy in Cu+Au collisions at $\sqrt{s_{NN}} = 200$ GeV,” *Phys. Rev.* **C98** no. 1, (2018) 014915, arXiv:1712.01332 [nucl-ex].
- [23] **Particle Data Group** Collaboration, C. Patrignani *et al.*, “Review of Particle Physics,” *Chin. Phys.* **C40** no. 10, (2016) 100001.
- [24] **STAR** Collaboration, B. I. Abelev *et al.*, “Global polarization measurement in Au+Au collisions,” *Phys. Rev.* **C76** (2007) 024915, arXiv:0705.1691 [nucl-ex]. [Erratum: *Phys. Rev.* **C95**,no.3,039906(2017)].
- [25] S. Wheaton and J. Cleymans, “THERMUS: A Thermal model package for ROOT,” *Comput. Phys. Commun.* **180** (2009) 84–106, arXiv:hep-ph/0407174 [hep-ph].
- [26] **ALICE** Collaboration, K. Aamodt *et al.*, “The ALICE experiment at the CERN LHC,” *JINST* **3** (2008) S08002.
- [27] **ALICE** Collaboration, B. B. Abelev *et al.*, “Performance of the ALICE Experiment at the CERN LHC,” *Int. J. Mod. Phys.* **A29** (2014) 1430044, arXiv:1402.4476 [nucl-ex].
- [28] **ALICE** Collaboration, G. Dellacasa *et al.*, “ALICE: Technical design report of the time projection chamber,” *CERN-OPEN-2000-183*, *CERN-LHCC-2000-001* (2000).
- [29] **ALICE** Collaboration, G. Dellacasa *et al.*, “ALICE technical design report of the inner tracking system (ITS),” *CERN-LHCC-99-12* (1999).
- [30] **ALICE** Collaboration, G. Dellacasa *et al.*, “ALICE technical design report of the zero degree calorimeter (ZDC),” *CERN-LHCC-99-05* (1999).
- [31] **ALICE** Collaboration, E. Abbas *et al.*, “Performance of the ALICE VZERO system,” *JINST* **8** (2013) P10016, arXiv:1306.3130 [nucl-ex].
- [32] **ALICE** Collaboration, K. Aamodt *et al.*, “Charged-particle multiplicity density at mid-rapidity in central Pb-Pb collisions at $\sqrt{s_{NN}} = 2.76$ TeV,” *Phys. Rev. Lett.* **105** (2010) 252301, arXiv:1011.3916 [nucl-ex].
- [33] **ALICE** Collaboration, K. Aamodt *et al.*, “Centrality dependence of the charged-particle multiplicity density at mid-rapidity in Pb-Pb collisions at $\sqrt{s_{NN}} = 2.76$ TeV,” *Phys. Rev. Lett.* **106** (2011) 032301, arXiv:1012.1657 [nucl-ex].
- [34] **ALICE** Collaboration, B. Abelev *et al.*, “Centrality determination of Pb-Pb collisions at $\sqrt{s_{NN}} = 2.76$ TeV with ALICE,” *Phys. Rev.* **C88** no. 4, (2013) 044909, arXiv:1301.4361 [nucl-ex].
- [35] I. Selyuzhenkov and S. Voloshin, “Effects of non-uniform acceptance in anisotropic flow measurement,” *Phys. Rev.* **C77** (2008) 034904, arXiv:0707.4672 [nucl-th].

- [36] A. M. Poskanzer and S. A. Voloshin, “Methods for analyzing anisotropic flow in relativistic nuclear collisions,” *Phys. Rev.* **C58** (1998) 1671–1678, arXiv:nucl-ex/9805001 [nucl-ex].
- [37] D. Macina and N. De Marco, “Modification IR2 to solve the ALICE ZDC-TCTVB interference problem,” *LHC-LJ-EC-0025* (2011) .
- [38] ALICE Collaboration, P. Cortese *et al.*, “ALICE technical design report on forward detectors: FMD, T0 and V0,” *CERN-LHCC-2004-025* (2004) .
- [39] ALICE Collaboration, S. Acharya *et al.*, “Anisotropic flow of identified particles in Pb-Pb collisions at $\sqrt{s_{NN}} = 5.02$ TeV,” *JHEP* **09** (2018) 006, arXiv:1805.04390 [nucl-ex].
- [40] R. Barlow, “Systematic errors: Facts and fictions,” in *Advanced Statistical Techniques in Particle Physics. Proceedings, Conference, Durham, UK, March 18-22, 2002*, pp. 134–144. 2002. arXiv:hep-ex/0207026 [hep-ex].
- [41] STAR Collaboration, I. Selyuzhenkov, “Acceptance effects in the hyperons global polarization measurement,” *AIP Conf. Proc.* **870** no. 1, (2006) 712–715, arXiv:nucl-ex/0608034 [nucl-ex].

A The ALICE Collaboration

S. Acharya¹⁴¹, D. Adamová⁹³, S.P. Adhya¹⁴¹, A. Adler⁷³, J. Adolfsson⁷⁹, M.M. Aggarwal⁹⁸, G. Aglieri Rinella³⁴, M. Agnello³¹, N. Agrawal^{10, 48, 53}, Z. Ahammed¹⁴¹, S. Ahmad¹⁷, S.U. Ahn⁷⁵, A. Akindinov⁹⁰, M. Al-Turany¹⁰⁵, S.N. Alam¹⁴¹, D.S.D. Albuquerque¹²², D. Aleksandrov⁸⁶, B. Alessandro⁵⁸, H.M. Alfanda⁶, R. Alfaro Molina⁷¹, B. Ali¹⁷, Y. Ali¹⁵, A. Alici^{10, 27, 53}, A. Alkin², J. Alme²², T. Alt⁶⁸, L. Altenkamper²², I. Altsybeev¹¹², M.N. Anaam⁶, C. Andrei⁴⁷, D. Andreou³⁴, H.A. Andrews¹⁰⁹, A. Andronic¹⁴⁴, M. Angeletti³⁴, V. Anguelov¹⁰², C. Anson¹⁶, T. Antičić¹⁰⁶, F. Antinori⁵⁶, P. Antonioli⁵³, R. Anwar¹²⁵, N. Apadula⁷⁸, L. Aphecetche¹¹⁴, H. Appelshäuser⁶⁸, S. Arcelli²⁷, R. Arnaldi⁵⁸, M. Arratia⁷⁸, I.C. Arsene²¹, M. Arslanok¹⁰², A. Augustinus³⁴, R. Auerbeck¹⁰⁵, S. Aziz⁶¹, M.D. Azmi¹⁷, A. Badalà⁵⁵, Y.W. Baek⁴⁰, S. Bagnasco⁵⁸, X. Bai¹⁰⁵, R. Bailhache⁶⁸, R. Bala⁹⁹, A. Baldisseri¹³⁷, M. Ball⁴², S. Balouza¹⁰³, R.C. Baral⁸⁴, R. Barbera²⁸, L. Barioglio²⁶, G.G. Barnaföldi¹⁴⁵, L.S. Barnby⁹², V. Barret¹³⁴, P. Bartalini⁶, K. Barth³⁴, E. Bartsch⁶⁸, F. Baruffaldi²⁹, N. Bastid¹³⁴, S. Basu¹⁴³, G. Batigne¹¹⁴, B. Batyunya⁷⁴, P.C. Batzing²¹, D. Bauri⁴⁸, J.L. Bazo Alba¹¹⁰, I.G. Bearden⁸⁷, C. Bedda⁶³, N.K. Behera⁶⁰, I. Belikov¹³⁶, F. Bellini³⁴, R. Bellwied¹²⁵, V. Belyaev⁹¹, G. Bencedi¹⁴⁵, S. Beole²⁶, A. Bercuci⁴⁷, Y. Berdnikov⁹⁶, D. Berenyi¹⁴⁵, R.A. Bertens¹³⁰, D. Berzano⁵⁸, M.G. Besoiu⁶⁷, L. Betev³⁴, A. Bhasin⁹⁹, I.R. Bhat⁹⁹, M.A. Bhat³, H. Bhatt⁴⁸, B. Bhattacharjee⁴¹, A. Bianchi²⁶, L. Bianchi²⁶, N. Bianchi⁵¹, J. Bielčik³⁷, J. Bielčíková⁹³, A. Bilandzic^{103, 117}, G. Biro¹⁴⁵, R. Biswas³, S. Biswas³, J.T. Blair¹¹⁹, D. Blau⁸⁶, C. Blume⁶⁸, G. Boca¹³⁹, F. Bock^{34, 94}, A. Bogdanov⁹¹, L. Boldizsár¹⁴⁵, A. Bolozdynya⁹¹, M. Bombara³⁸, G. Bonomi¹⁴⁰, H. Borel¹³⁷, A. Borissov^{91, 144}, M. Borri¹²⁷, H. Bossi¹⁴⁶, E. Botta²⁶, L. Bratrud⁶⁸, P. Braun-Munzinger¹⁰⁵, M. Bregant¹²¹, T.A. Broker⁶⁸, M. Broz³⁷, E.J. Brucken⁴³, E. Bruna⁵⁸, G.E. Bruno^{33, 104}, M.D. Buckland¹²⁷, D. Budnikov¹⁰⁷, H. Buesching⁶⁸, S. Bufalino³¹, O. Bugnon¹¹⁴, P. Buhler¹¹³, P. Buncic³⁴, Z. Buthelezi⁷², J.B. Butt¹⁵, J.T. Buxton⁹⁵, S.A. Bysiak¹¹⁸, D. Caffarri⁸⁸, A. Caliva¹⁰⁵, E. Calvo Villar¹¹⁰, R.S. Camacho⁴⁴, P. Camerini²⁵, A.A. Capon¹¹³, F. Carnesecchi^{10, 27}, J. Castillo Castellanos¹³⁷, A.J. Castro¹³⁰, E.A.R. Casula⁵⁴, F. Catalano³¹, C. Ceballos Sanchez⁵², P. Chakraborty⁴⁸, S. Chandra¹⁴¹, B. Chang¹²⁶, W. Chang⁶, S. Chapeland³⁴, M. Chartier¹²⁷, S. Chattopadhyay¹⁴¹, S. Chattopadhyay¹⁰⁸, A. Chauvin²⁴, C. Cheshkov¹³⁵, B. Cheynis¹³⁵, V. Chibante Barroso³⁴, D.D. Chinellato¹²², S. Cho⁶⁰, P. Chochula³⁴, T. Chowdhury¹³⁴, P. Christakoglou⁸⁸, C.H. Christensen⁸⁷, P. Christiansen⁷⁹, T. Chujo¹³³, C. Cicalo⁵⁴, L. Cifarelli^{10, 27}, F. Cindolo⁵³, J. Cleymans¹²⁴, F. Colamaria⁵², D. Colella⁵², A. Collu⁷⁸, M. Colocci²⁷, M. Concas^{58, ii}, G. Conesa Balbastre⁷⁷, Z. Conesa del Valle⁶¹, G. Contin^{59, 127}, J.G. Contreras³⁷, T.M. Cormier⁹⁴, Y. Corrales Morales^{26, 58}, P. Cortese³², M.R. Cosentino¹²³, F. Costa³⁴, S. Costanza¹³⁹, P. Crochet¹³⁴, E. Cuautele⁶⁹, P. Cui⁶, L. Cunqueiro⁹⁴, D. Dabrowski¹⁴², T. Dahms^{103, 117}, A. Dainese⁵⁶, F.P.A. Damas^{114, 137}, S. Dani⁶⁵, M.C. Danisch¹⁰², A. Danu⁶⁷, D. Das¹⁰⁸, I. Das¹⁰⁸, P. Das³, S. Das³, A. Dash⁸⁴, S. Dash⁴⁸, A. Dashi¹⁰³, S. De^{49, 84}, A. De Caro³⁰, G. de Cataldo⁵², C. de Conti¹²¹, J. de Cuveland³⁹, A. De Falco²⁴, D. De Gruttola¹⁰, N. De Marco⁵⁸, S. De Pasquale³⁰, R.D. De Souza¹²², S. Deb⁴⁹, H.F. Degenhardt¹²¹, K.R. Deja¹⁴², A. Deloff⁸³, S. Delsanto^{26, 131}, D. Devetak¹⁰⁵, P. Dhankher⁴⁸, D. Di Bari³³, A. Di Mauro³⁴, R.A. Diaz⁸, T. Dietel¹²⁴, P. Dillenseger⁶⁸, Y. Ding⁶, R. Divia³⁴, Ø. Djuvsland²², U. Dmitrieva⁶², A. Dobrin^{34, 67}, B. Dönigus⁶⁸, O. Dordic²¹, A.K. Dubey¹⁴¹, A. Dubla¹⁰⁵, S. Dudi⁹⁸, M. Dukhishyam⁸⁴, P. Dupieux¹³⁴, R.J. Ehlers¹⁴⁶, D. Elia⁵², H. Engel⁷³, E. Eppe¹⁴⁶, B. Erazmus¹¹⁴, F. Erhardt⁹⁷, A. Erokhin¹¹², M.R. Ersdal²², B. Espagnon⁶¹, G. Eulisse³⁴, J. Eum¹⁸, D. Evans¹⁰⁹, S. Evdokimov⁸⁹, L. Fabbietti^{103, 117}, M. Faggin²⁹, J. Faivre⁷⁷, F. Fan⁶, A. Fantoni⁵¹, M. Fasel⁹⁴, P. Fecchio³¹, A. Feliciello⁵⁸, G. Feofilov¹¹², A. Fernández Téllez⁴⁴, A. Ferrero¹³⁷, A. Ferretti²⁶, A. Festanti³⁴, V.J.G. Feuillard¹⁰², J. Figiel¹¹⁸, S. Filchagin¹⁰⁷, D. Finogeev⁶², F.M. Fionda²², G. Fiorenza⁵², F. Flor¹²⁵, S. Foertsch⁷², P. Foka¹⁰⁵, S. Fokin⁸⁶, E. Fragiaco⁵⁹, U. Frankfeld¹⁰⁵, G.G. Fronze²⁶, U. Fuchs³⁴, C. Furget⁷⁷, A. Furs⁶², M. Fusco Girard³⁰, J.J. Gaardhøje⁸⁷, M. Gagliardi²⁶, A.M. Gago¹¹⁰, A. Gal¹³⁶, C.D. Galvan¹²⁰, P. Ganoti⁸², C. Garabatos¹⁰⁵, E. Garcia-Solis¹¹, K. Garg²⁸, C. Gargiulo³⁴, A. Garibli⁸⁵, K. Garner¹⁴⁴, P. Gasik^{103, 117}, E.F. Gauger¹¹⁹, M.B. Gay Ducati⁷⁰, M. Germain¹¹⁴, J. Ghosh¹⁰⁸, P. Ghosh¹⁴¹, S.K. Ghosh³, P. Gianotti⁵¹, P. Giubellino^{58, 105}, P. Giubilato²⁹, P. Glässel¹⁰², D.M. Gómez Coral⁷¹, A. Gomez Ramirez⁷³, V. Gonzalez¹⁰⁵, P. González-Zamora⁴⁴, S. Gorbunov³⁹, L. Görlich¹¹⁸, S. Gotovac³⁵, V. Grabski⁷¹, L.K. Graczykowski¹⁴², K.L. Graham¹⁰⁹, L. Greiner⁷⁸, A. Grelli⁶³, C. Grigoras³⁴, V. Grigoriev⁹¹, A. Grigoryan¹, S. Grigoryan⁷⁴, O.S. Groettkvick²², F. Grosa³¹, J.F. Grosse-Oetringhaus³⁴, R. Grosso¹⁰⁵, R. Guernane⁷⁷, B. Guerzoni²⁷, M. Guittiere¹¹⁴, K. Gulbrandsen⁸⁷, T. Gunji¹³², A. Gupta⁹⁹, R. Gupta⁹⁹, I.B. Guzman⁴⁴, R. Haake¹⁴⁶, M.K. Habib¹⁰⁵, C. Hadjidakis⁶¹, H. Hamagaki⁸⁰, G. Hamar¹⁴⁵, M. Hamid⁶, R. Hannigan¹¹⁹, M.R. Haque⁶³, A. Harlanderova¹⁰⁵, J.W. Harris¹⁴⁶, A. Harton¹¹, J.A. Hasenbichler³⁴, H. Hassan⁷⁷, D. Hatzifotiadou^{10, 53}, P. Hauer⁴², S. Hayashi¹³², A.D.L.B. Hechavarria¹⁴⁴, S.T. Heckel⁶⁸, E. Hellbär⁶⁸, H. Helstrup³⁶, A. Herghelegiu⁴⁷, E.G. Hernandez⁴⁴, G. Herrera Corral⁹, F. Herrmann¹⁴⁴, K.F. Hetland³⁶, T.E. Hilden⁴³, H. Hillemanns³⁴, C. Hills¹²⁷, B. Hippolyte¹³⁶, B. Hohlweger¹⁰³, D. Horak³⁷, S. Hornung¹⁰⁵, R. Hosokawa^{16, 133}, P. Hristov³⁴, C. Huang⁶¹,

C. Hughes¹³⁰, P. Huhn⁶⁸, T.J. Humanic⁹⁵, H. Hushnud¹⁰⁸, L.A. Husova¹⁴⁴, N. Hussain⁴¹, S.A. Hussain¹⁵, D. Hutter³⁹, D.S. Hwang¹⁹, J.P. Iddon^{34,127}, R. Ilkaev¹⁰⁷, M. Inaba¹³³, M. Ippolitov⁸⁶, M.S. Islam¹⁰⁸, M. Ivanov¹⁰⁵, V. Ivanov⁹⁶, V. Izucheev⁸⁹, B. Jacak⁷⁸, N. Jacazio^{27,53}, P.M. Jacobs⁷⁸, M.B. Jadhav⁴⁸, S. Jadlovská¹¹⁶, J. Jadlovsky¹¹⁶, S. Jaelani⁶³, C. Jahnke¹²¹, M.J. Jakubowska¹⁴², M.A. Janik¹⁴², M. Jercic⁹⁷, O. Jevons¹⁰⁹, R.T. Jimenez Bustamante¹⁰⁵, M. Jin¹²⁵, F. Jonas^{94,144}, P.G. Jones¹⁰⁹, A. Jusko¹⁰⁹, P. Kalinak⁶⁴, A. Kalweit³⁴, J.H. Kang¹⁴⁷, V. Kaplin⁹¹, S. Kar⁶, A. Karasu Uysal⁷⁶, O. Karavichev⁶², T. Karavicheva⁶², P. Karczmarczyk³⁴, E. Karpechev⁶², U. Kebschull⁷³, R. Keidel⁴⁶, M. Keil³⁴, B. Ketzer⁴², Z. Khabanova⁸⁸, A.M. Khan⁶, S. Khan¹⁷, S.A. Khan¹⁴¹, A. Khanzadeev⁹⁶, Y. Kharlov⁸⁹, A. Khatun¹⁷, A. Khuntia^{49,118}, B. Kileng³⁶, B. Kim⁶⁰, B. Kim¹³³, D. Kim¹⁴⁷, D.J. Kim¹²⁶, E.J. Kim¹³, H. Kim¹⁴⁷, J. Kim¹⁴⁷, J.S. Kim⁴⁰, J. Kim¹⁰², J. Kim¹⁴⁷, J. Kim¹³, M. Kim¹⁰², S. Kim¹⁹, T. Kim¹⁴⁷, T. Kim¹⁴⁷, S. Kirsch³⁹, I. Kisel³⁹, S. Kiselev⁹⁰, A. Kisiel¹⁴², J.L. Klay⁵, C. Klein⁶⁸, J. Klein⁵⁸, S. Klein⁷⁸, C. Klein-Bösing¹⁴⁴, S. Klewin¹⁰², A. Kluge³⁴, M.L. Knichel³⁴, A.G. Knospe¹²⁵, C. Kobdaj¹¹⁵, M.K. Köhler¹⁰², T. Kollegger¹⁰⁵, A. Kondratyev⁷⁴, N. Kondratyeva⁹¹, E. Kondratyuk⁸⁹, P.J. Konopka³⁴, L. Koska¹¹⁶, O. Kovalenko⁸³, V. Kovalenko¹¹², M. Kowalski¹¹⁸, I. Králik⁶⁴, A. Kravčáková³⁸, L. Kreis¹⁰⁵, M. Krivda^{64,109}, F. Krizek⁹³, K. Krizkova Gajdosova³⁷, M. Krüger⁶⁸, E. Kryshen⁹⁶, M. Krzewicki³⁹, A.M. Kubera⁹⁵, V. Kučera⁶⁰, C. Kuhn¹³⁶, P.G. Kuijper⁸⁸, L. Kumar⁹⁸, S. Kumar⁴⁸, S. Kundu⁸⁴, P. Kurashvili⁸³, A. Kurepin⁶², A.B. Kurepin⁶², A. Kuryakin¹⁰⁷, S. Kushpil⁹³, J. Kvapil¹⁰⁹, M.J. Kweon⁶⁰, J.Y. Kwon⁶⁰, Y. Kwon¹⁴⁷, S.L. La Pointe³⁹, P. La Rocca²⁸, Y.S. Lai⁷⁸, R. Langoy¹²⁹, K. Lapidus^{34,146}, A. Lardeux²¹, P. Larionov⁵¹, E. Laudi³⁴, R. Lavicka³⁷, T. Lazareva¹¹², R. Lea²⁵, L. Leardini¹⁰², S. Lee¹⁴⁷, F. Lehas⁸⁸, S. Lehner¹¹³, J. Lehrbach³⁹, R.C. Lemmon⁹², I. León Monzón¹²⁰, E.D. Lesser²⁰, M. Lettrich³⁴, P. Lévai¹⁴⁵, X. Li¹², X.L. Li⁶, J. Lien¹²⁹, R. Lietava¹⁰⁹, B. Lim¹⁸, S. Lindal²¹, V. Lindenstruth³⁹, S.W. Lindsay¹²⁷, C. Lippmann¹⁰⁵, M.A. Lisa⁹⁵, V. Litichevskiy⁴³, A. Liu⁷⁸, S. Liu⁹⁵, W.J. Llope¹⁴³, I.M. Lofnes²², V. Loginov⁹¹, C. Loizides⁹⁴, P. Loncar³⁵, X. Lopez¹³⁴, E. López Torres⁸, P. Luettig⁶⁸, J.R. Luhder¹⁴⁴, M. Lunardon²⁹, G. Luparello⁵⁹, A. Maevskaya⁶², M. Mager³⁴, S.M. Mahmood²¹, T. Mahmoud⁴², A. Maire¹³⁶, R.D. Majka¹⁴⁶, M. Malaev⁹⁶, Q.W. Malik²¹, L. Malinina^{74,iii}, D. Mal'Kevich⁹⁰, P. Malzacher¹⁰⁵, G. Mandaglio⁵⁵, V. Manko⁸⁶, F. Manso¹³⁴, V. Manzari⁵², Y. Mao⁶, M. Marchisone¹³⁵, J. Mareš⁶⁶, G.V. Margagliotti²⁵, A. Margotti⁵³, J. Margutti⁶³, A. Marín¹⁰⁵, C. Markert¹¹⁹, M. Marquard⁶⁸, N.A. Martin¹⁰², P. Martinengo³⁴, J.L. Martinez¹²⁵, M.I. Martínez⁴⁴, G. Martínez García¹¹⁴, M. Martinez Pedreira³⁴, S. Masciocchi¹⁰⁵, M. Masera²⁶, A. Masoni⁵⁴, L. Massacrier⁶¹, E. Masson¹¹⁴, A. Mastroserio^{52,138}, A.M. Mathis^{103,117}, O. Matonoha⁷⁹, P.F.T. Matuoka¹²¹, A. Matyja¹¹⁸, C. Mayer¹¹⁸, M. Mazzilli³³, M.A. Mazzoni⁵⁷, A.F. Mechler⁶⁸, F. Meddi²³, Y. Melikyan^{62,91}, A. Menchaca-Rocha⁷¹, C. Mengke⁶, E. Meninno³⁰, M. Meres¹⁴, S. Mhlanga¹²⁴, Y. Miake¹³³, L. Micheletti²⁶, M.M. Mieskolainen⁴³, D.L. Mihaylov¹⁰³, K. Mikhaylov^{74,90}, A. Mischke^{63,i}, A.N. Mishra⁶⁹, D. Miśkowiec¹⁰⁵, C.M. Mitu⁶⁷, A. Modak³, N. Mohammadi³⁴, A.P. Mohanty⁶³, B. Mohanty⁸⁴, M. Mohisin Khan^{17,iv}, M. Mondal¹⁴¹, C. Mordasini¹⁰³, D.A. Moreira De Godoy¹⁴⁴, L.A.P. Moreno⁴⁴, S. Moretto²⁹, A. Morreale¹¹⁴, A. Morsch³⁴, T. Mrnjavac³⁴, V. Muccifora⁵¹, E. Mudnic³⁵, D. Mühlheim¹⁴⁴, S. Muhuri¹⁴¹, J.D. Mulligan⁷⁸, M.G. Munhoz¹²¹, K. Münnig⁴², R.H. Munzer⁶⁸, H. Murakami¹³², S. Murray¹²⁴, L. Musa³⁴, J. Musinsky⁶⁴, C.J. Myers¹²⁵, J.W. Myrcha¹⁴², B. Naik⁴⁸, R. Nair⁸³, B.K. Nandi⁴⁸, R. Nania^{10,53}, E. Nappi⁵², M.U. Naru¹⁵, A.F. Nassirpour⁷⁹, H. Natal da Luz¹²¹, C. Natrass¹³⁰, R. Nayak⁴⁸, T.K. Nayak^{84,141}, S. Nazarenko¹⁰⁷, A. Neagu²¹, R.A. Negrao De Oliveira⁶⁸, L. Nellen⁶⁹, S.V. Nesbo³⁶, G. Neskovic³⁹, D. Nesterov¹¹², B.S. Nielsen⁸⁷, S. Nikolaev⁸⁶, S. Nikulin⁸⁶, V. Nikulin⁹⁶, F. Noferini^{10,53}, P. Nomokonov⁷⁴, G. Nooren⁶³, J. Norman⁷⁷, N. Novitzky¹³³, P. Nowakowski¹⁴², A. Nyanin⁸⁶, J. Nystrand²², M. Ogino⁸⁰, A. Ohlson¹⁰², J. Olieni¹⁴², A.C. Oliveira Da Silva¹²¹, M.H. Oliver¹⁴⁶, C. Oppedisano⁵⁸, R. Orava⁴³, A. Ortiz Velasquez⁶⁹, A. Oskarsson⁷⁹, J. Otwinowski¹¹⁸, K. Oyama⁸⁰, Y. Pachmayer¹⁰², V. Pacik⁸⁷, D. Pagano¹⁴⁰, G. Paic⁶⁹, P. Palni⁶, J. Pan¹⁴³, A.K. Pandey⁴⁸, S. Panebianco¹³⁷, P. Pareek⁴⁹, J. Park⁶⁰, J.E. Parkkila¹²⁶, S. Parmar⁹⁸, S.P. Pathak¹²⁵, R.N. Patra¹⁴¹, B. Paul^{24,58}, H. Pei⁶, T. Peitzmann⁶³, X. Peng⁶, L.G. Pereira⁷⁰, H. Pereira Da Costa¹³⁷, D. Peresunko⁸⁶, G.M. Perez⁸, E. Perez Lezama⁶⁸, V. Peskov⁶⁸, Y. Pestov⁴, V. Petráček³⁷, M. Petrovici⁴⁷, R.P. Pezzi⁷⁰, S. Piano⁵⁹, M. Pikna¹⁴, P. Pillot¹¹⁴, L.O.D.L. Pimentel⁸⁷, O. Pinazza^{34,53}, L. Pinsky¹²⁵, C. Pinto²⁸, S. Pisano⁵¹, D. Pistone⁵⁵, D.B. Piyarathna¹²⁵, M. Płoskoń⁷⁸, M. Planinic⁹⁷, F. Pliquett⁶⁸, J. Pluta¹⁴², S. Pochybova¹⁴⁵, M.G. Poghossyan⁹⁴, B. Polichtchouk⁸⁹, N. Poljak⁹⁷, A. Pop⁴⁷, H. Poppenborg¹⁴⁴, S. Porteboeuf-Houssais¹³⁴, V. Pozdniakov⁷⁴, S.K. Prasad³, R. Preghenella⁵³, F. Prino⁵⁸, C.A. Pruneau¹⁴³, I. Pshenichnov⁶², M. Puccio^{26,34}, V. Punin¹⁰⁷, K. Puranapanda¹⁴¹, J. Putschke¹⁴³, R.E. Quishpe¹²⁵, S. Ragoni¹⁰⁹, S. Raha³, S. Rajput⁹⁹, J. Rak¹²⁶, A. Rakotozafindrabe¹³⁷, L. Ramello³², F. Rami¹³⁶, R. Raniwala¹⁰⁰, S. Raniwala¹⁰⁰, S.S. Räsänen⁴³, B.T. Rascanu⁶⁸, R. Rath⁴⁹, V. Ratza⁴², I. Ravasenga³¹, K.F. Read^{94,130}, K. Redlich^{83,v}, A. Rehman²², P. Reichelt⁶⁸, F. Reidt³⁴, X. Ren⁶, R. Renfordt⁶⁸, A. Reshetin⁶², J.-P. Revol¹⁰, K. Reygers¹⁰², V. Riabov⁹⁶, T. Richert^{79,87}, M. Richter²¹, P. Riedler³⁴, W. Riegler³⁴, F. Riggi²⁸, C. Ristea⁶⁷, S.P. Rode⁴⁹, M. Rodríguez Cahuantzi⁴⁴, K. Røed²¹,

R. Rogalev⁸⁹, E. Rogochaya⁷⁴, D. Rohr³⁴, D. Röhrich²², P.S. Rokita¹⁴², F. Ronchetti⁵¹, E.D. Rosas⁶⁹, K. Roslon¹⁴², P. Rosnet¹³⁴, A. Rossi^{29,56}, A. Rotondi¹³⁹, F. Roukoutakis⁸², A. Roy⁴⁹, P. Roy¹⁰⁸, O.V. Rueda⁷⁹, R. Rui²⁵, B. Rumyantsev⁷⁴, A. Rustamov⁸⁵, E. Ryabinkin⁸⁶, Y. Ryabov⁹⁶, A. Rybicki¹¹⁸, H. Ryttonen¹²⁶, S. Sadhu¹⁴¹, S. Sadovsky⁸⁹, K. Šafařík^{34,37}, S.K. Saha¹⁴¹, B. Sahoo⁴⁸, P. Sahoo^{48,49}, R. Sahoo⁴⁹, S. Sahoo⁶⁵, P.K. Sahu⁶⁵, J. Saini¹⁴¹, S. Sakai¹³³, S. Sambyal⁹⁹, V. Samsonov^{91,96}, F.R. Sanchez⁴⁴, A. Sandoval⁷¹, A. Sarkar⁷², D. Sarkar¹⁴³, N. Sarkar¹⁴¹, P. Sarma⁴¹, V.M. Sarti¹⁰³, M.H.P. Sas⁶³, E. Scapparone⁵³, B. Schaefer⁹⁴, J. Schambach¹¹⁹, H.S. Scheid⁶⁸, C. Schiaua⁴⁷, R. Schicker¹⁰², A. Schmah¹⁰², C. Schmidt¹⁰⁵, H.R. Schmidt¹⁰¹, M.O. Schmidt¹⁰², M. Schmidt¹⁰¹, N.V. Schmidt^{68,94}, A.R. Schmier¹³⁰, J. Schukraft^{34,87}, Y. Schutz^{34,136}, K. Schwarz¹⁰⁵, K. Schweda¹⁰⁵, G. Scioli²⁷, E. Scomparin⁵⁸, M. Šefčík³⁸, J.E. Seger¹⁶, Y. Sekiguchi¹³², D. Sekihata^{45,132}, I. Selyuzhenkov^{91,105}, S. Senyukov¹³⁶, D. Serebryakov⁶², E. Serradilla⁷¹, P. Sett⁴⁸, A. Sevcenco⁶⁷, A. Shabanov⁶², A. Shabetai¹¹⁴, R. Shahoyan³⁴, W. Shaikh¹⁰⁸, A. Shangaraev⁸⁹, A. Sharma⁹⁸, A. Sharma⁹⁹, H. Sharma¹¹⁸, M. Sharma⁹⁹, N. Sharma⁹⁸, A.I. Sheikh¹⁴¹, K. Shigaki⁴⁵, M. Shimomura⁸¹, S. Shirinkin⁹⁰, Q. Shou¹¹¹, Y. Sibiriak⁸⁶, S. Siddhanta⁵⁴, T. Siemiarczuk⁸³, D. Silvermyr⁷⁹, C. Silvestre⁷⁷, G. Simatovic⁸⁸, G. Simonetti^{34,103}, R. Singh⁸⁴, R. Singh⁹⁹, V.K. Singh¹⁴¹, V. Singhal¹⁴¹, T. Sinha¹⁰⁸, B. Sitar¹⁴, M. Sitta³², T.B. Skaali²¹, M. Slupecki¹²⁶, N. Smirnov¹⁴⁶, R.J.M. Snellings⁶³, T.W. Snellman^{43,126}, J. Sochan¹¹⁶, C. Soncco¹¹⁰, J. Song^{60,125}, A. Songmoolnak¹¹⁵, F. Soramel²⁹, S. Sorensen¹³⁰, I. Sputowska¹¹⁸, J. Stachel¹⁰², I. Stan⁶⁷, P. Stankus⁹⁴, P.J. Steffanic¹³⁰, E. Stenlund⁷⁹, D. Stocco¹¹⁴, M.M. Storetvedt³⁶, P. Strmen¹⁴, A.A.P. Suaide¹²¹, T. Sugitate⁴⁵, C. Suire⁶¹, M. Suleymanov¹⁵, M. Suljic³⁴, R. Sultanov⁹⁰, M. Šumbera⁹³, S. Sumowidagdo⁵⁰, K. Suzuki¹¹³, S. Swain⁶⁵, A. Szabo¹⁴, I. Szarka¹⁴, U. Tabassam¹⁵, G. Taillepie¹³⁴, J. Takahashi¹²², G.J. Tambave²², S. Tang^{6,134}, M. Tarhini¹¹⁴, M.G. Tarzila⁴⁷, A. Tauro³⁴, G. Tejada Muñoz⁴⁴, A. Telesca³⁴, C. Terrevoli^{29,125}, D. Thakur⁴⁹, S. Thakur¹⁴¹, D. Thomas¹¹⁹, F. Thoresen⁸⁷, R. Tieulent¹³⁵, A. Tikhonov⁶², A.R. Timmins¹²⁵, A. Toia⁶⁸, N. Topilskaya⁶², M. Toppi⁵¹, F. Torres-Acosta²⁰, S.R. Torres¹²⁰, A. Trifiro⁵⁵, S. Tripathy⁴⁹, T. Tripathy⁴⁸, S. Trogolo²⁹, G. Trombetta³³, L. Tropp³⁸, V. Trubnikov², W.H. Trzaska¹²⁶, T.P. Trzcinski¹⁴², B.A. Trzeciak⁶³, T. Tsuji¹³², A. Tumkin¹⁰⁷, R. Turrisi⁵⁶, T.S. Tveter²¹, K. Ullaland²², E.N. Umaka¹²⁵, A. Uras¹³⁵, G.L. Usai²⁴, A. Utrobicic⁹⁷, M. Vala^{38,116}, N. Valle¹³⁹, S. Vallero⁵⁸, N. van der Kolk⁶³, L.V.R. van Doremalen⁶³, M. van Leeuwen⁶³, P. Vande Vyvre³⁴, D. Varga¹⁴⁵, Z. Varga¹⁴⁵, M. Varga-Kofarago¹⁴⁵, A. Vargas⁴⁴, M. Vargyas¹²⁶, R. Varma⁴⁸, M. Vasileiou⁸², A. Vasiliev⁸⁶, O. Vázquez Doce^{103,117}, V. Vechernin¹¹², A.M. Veen⁶³, E. Vercellin²⁶, S. Vergara Limón⁴⁴, L. Vermunt⁶³, R. Vernet⁷, R. Vértesi¹⁴⁵, M.G.D.L.C. Vicencio⁹, L. Vickovic³⁵, J. Viinikainen¹²⁶, Z. Vilakazi¹³¹, O. Villalobos Baillie¹⁰⁹, A. Villatoro Tello⁴⁴, G. Vino⁵², A. Vinogradov⁸⁶, T. Virgili³⁰, V. Vislavicius⁸⁷, A. Vodopyanov⁷⁴, B. Volkel³⁴, M.A. Völkl¹⁰¹, K. Voloshin⁹⁰, S.A. Voloshin¹⁴³, G. Volpe³³, B. von Haller³⁴, I. Vorobyev¹⁰³, D. Voscek¹¹⁶, J. Vrláková³⁸, B. Wagner²², M. Weber¹¹³, S.G. Weber^{105,144}, A. Wegrzynek³⁴, D.F. Weiser¹⁰², S.C. Wenzel³⁴, J.P. Wessels¹⁴⁴, E. Widmann¹¹³, J. Wiechula⁶⁸, J. Wikne²¹, G. Wilk⁸³, J. Wilkinson⁵³, G.A. Willems³⁴, E. Willsher¹⁰⁹, B. Windelband¹⁰², W.E. Witt¹³⁰, Y. Wu¹²⁸, R. Xu⁶, S. Yalcin⁷⁶, K. Yamakawa⁴⁵, S. Yang²², S. Yano¹³⁷, Z. Yin⁶, H. Yokoyama^{63,133}, I.-K. Yoo¹⁸, J.H. Yoon⁶⁰, S. Yuan²², A. Yuncu¹⁰², V. Yurchenko², V. Zaccolo^{25,58}, A. Zaman¹⁵, C. Zampolli³⁴, H.J.C. Zanoli^{63,121}, N. Zardoshti³⁴, A. Zarochentsev¹¹², P. Závada⁶⁶, N. Zaviyalov¹⁰⁷, H. Zbroszczyk¹⁴², M. Zhalov⁹⁶, X. Zhang⁶, Z. Zhang⁶, C. Zhao²¹, V. Zherebchevskii¹¹², N. Zhigareva⁹⁰, D. Zhou⁶, Y. Zhou⁸⁷, Z. Zhou²², J. Zhu⁶, Y. Zhu⁶, A. Zichichi^{10,27}, M.B. Zimmermann³⁴, G. Zinovjev², N. Zurlo¹⁴⁰,

Affiliation notes

ⁱ Deceased

ⁱⁱ Dipartimento DET del Politecnico di Torino, Turin, Italy

ⁱⁱⁱ M.V. Lomonosov Moscow State University, D.V. Skobeltsyn Institute of Nuclear Physics, Moscow, Russia

^{iv} Department of Applied Physics, Aligarh Muslim University, Aligarh, India

^v Institute of Theoretical Physics, University of Wrocław, Poland

Collaboration Institutes

¹ A.I. Alikhanyan National Science Laboratory (Yerevan Physics Institute) Foundation, Yerevan, Armenia

² Bogolyubov Institute for Theoretical Physics, National Academy of Sciences of Ukraine, Kiev, Ukraine

³ Bose Institute, Department of Physics and Centre for Astroparticle Physics and Space Science (CAPSS), Kolkata, India

⁴ Budker Institute for Nuclear Physics, Novosibirsk, Russia

⁵ California Polytechnic State University, San Luis Obispo, California, United States

- 6 Central China Normal University, Wuhan, China
- 7 Centre de Calcul de l'IN2P3, Villeurbanne, Lyon, France
- 8 Centro de Aplicaciones Tecnológicas y Desarrollo Nuclear (CEADEN), Havana, Cuba
- 9 Centro de Investigación y de Estudios Avanzados (CINVESTAV), Mexico City and Mérida, Mexico
- 10 Centro Fermi - Museo Storico della Fisica e Centro Studi e Ricerche "Enrico Fermi", Rome, Italy
- 11 Chicago State University, Chicago, Illinois, United States
- 12 China Institute of Atomic Energy, Beijing, China
- 13 Chonbuk National University, Jeonju, Republic of Korea
- 14 Comenius University Bratislava, Faculty of Mathematics, Physics and Informatics, Bratislava, Slovakia
- 15 COMSATS University Islamabad, Islamabad, Pakistan
- 16 Creighton University, Omaha, Nebraska, United States
- 17 Department of Physics, Aligarh Muslim University, Aligarh, India
- 18 Department of Physics, Pusan National University, Pusan, Republic of Korea
- 19 Department of Physics, Sejong University, Seoul, Republic of Korea
- 20 Department of Physics, University of California, Berkeley, California, United States
- 21 Department of Physics, University of Oslo, Oslo, Norway
- 22 Department of Physics and Technology, University of Bergen, Bergen, Norway
- 23 Dipartimento di Fisica dell'Università 'La Sapienza' and Sezione INFN, Rome, Italy
- 24 Dipartimento di Fisica dell'Università and Sezione INFN, Cagliari, Italy
- 25 Dipartimento di Fisica dell'Università and Sezione INFN, Trieste, Italy
- 26 Dipartimento di Fisica dell'Università and Sezione INFN, Turin, Italy
- 27 Dipartimento di Fisica e Astronomia dell'Università and Sezione INFN, Bologna, Italy
- 28 Dipartimento di Fisica e Astronomia dell'Università and Sezione INFN, Catania, Italy
- 29 Dipartimento di Fisica e Astronomia dell'Università and Sezione INFN, Padova, Italy
- 30 Dipartimento di Fisica 'E.R. Caianiello' dell'Università and Gruppo Collegato INFN, Salerno, Italy
- 31 Dipartimento DISAT del Politecnico and Sezione INFN, Turin, Italy
- 32 Dipartimento di Scienze e Innovazione Tecnologica dell'Università del Piemonte Orientale and INFN Sezione di Torino, Alessandria, Italy
- 33 Dipartimento Interateneo di Fisica 'M. Merlin' and Sezione INFN, Bari, Italy
- 34 European Organization for Nuclear Research (CERN), Geneva, Switzerland
- 35 Faculty of Electrical Engineering, Mechanical Engineering and Naval Architecture, University of Split, Split, Croatia
- 36 Faculty of Engineering and Science, Western Norway University of Applied Sciences, Bergen, Norway
- 37 Faculty of Nuclear Sciences and Physical Engineering, Czech Technical University in Prague, Prague, Czech Republic
- 38 Faculty of Science, P.J. Šafárik University, Košice, Slovakia
- 39 Frankfurt Institute for Advanced Studies, Johann Wolfgang Goethe-Universität Frankfurt, Frankfurt, Germany
- 40 Gangneung-Wonju National University, Gangneung, Republic of Korea
- 41 Gauhati University, Department of Physics, Guwahati, India
- 42 Helmholtz-Institut für Strahlen- und Kernphysik, Rheinische Friedrich-Wilhelms-Universität Bonn, Bonn, Germany
- 43 Helsinki Institute of Physics (HIP), Helsinki, Finland
- 44 High Energy Physics Group, Universidad Autónoma de Puebla, Puebla, Mexico
- 45 Hiroshima University, Hiroshima, Japan
- 46 Hochschule Worms, Zentrum für Technologietransfer und Telekommunikation (ZTT), Worms, Germany
- 47 Horia Hulubei National Institute of Physics and Nuclear Engineering, Bucharest, Romania
- 48 Indian Institute of Technology Bombay (IIT), Mumbai, India
- 49 Indian Institute of Technology Indore, Indore, India
- 50 Indonesian Institute of Sciences, Jakarta, Indonesia
- 51 INFN, Laboratori Nazionali di Frascati, Frascati, Italy
- 52 INFN, Sezione di Bari, Bari, Italy
- 53 INFN, Sezione di Bologna, Bologna, Italy
- 54 INFN, Sezione di Cagliari, Cagliari, Italy
- 55 INFN, Sezione di Catania, Catania, Italy
- 56 INFN, Sezione di Padova, Padova, Italy

- 57 INFN, Sezione di Roma, Rome, Italy
- 58 INFN, Sezione di Torino, Turin, Italy
- 59 INFN, Sezione di Trieste, Trieste, Italy
- 60 Inha University, Incheon, Republic of Korea
- 61 Institut de Physique Nucléaire d’Orsay (IPNO), Institut National de Physique Nucléaire et de Physique des Particules (IN2P3/CNRS), Université de Paris-Sud, Université Paris-Saclay, Orsay, France
- 62 Institute for Nuclear Research, Academy of Sciences, Moscow, Russia
- 63 Institute for Subatomic Physics, Utrecht University/Nikhef, Utrecht, Netherlands
- 64 Institute of Experimental Physics, Slovak Academy of Sciences, Košice, Slovakia
- 65 Institute of Physics, Homi Bhabha National Institute, Bhubaneswar, India
- 66 Institute of Physics of the Czech Academy of Sciences, Prague, Czech Republic
- 67 Institute of Space Science (ISS), Bucharest, Romania
- 68 Institut für Kernphysik, Johann Wolfgang Goethe-Universität Frankfurt, Frankfurt, Germany
- 69 Instituto de Ciencias Nucleares, Universidad Nacional Autónoma de México, Mexico City, Mexico
- 70 Instituto de Física, Universidade Federal do Rio Grande do Sul (UFRGS), Porto Alegre, Brazil
- 71 Instituto de Física, Universidad Nacional Autónoma de México, Mexico City, Mexico
- 72 iThemba LABS, National Research Foundation, Somerset West, South Africa
- 73 Johann-Wolfgang-Goethe Universität Frankfurt Institut für Informatik, Fachbereich Informatik und Mathematik, Frankfurt, Germany
- 74 Joint Institute for Nuclear Research (JINR), Dubna, Russia
- 75 Korea Institute of Science and Technology Information, Daejeon, Republic of Korea
- 76 KTO Karatay University, Konya, Turkey
- 77 Laboratoire de Physique Subatomique et de Cosmologie, Université Grenoble-Alpes, CNRS-IN2P3, Grenoble, France
- 78 Lawrence Berkeley National Laboratory, Berkeley, California, United States
- 79 Lund University Department of Physics, Division of Particle Physics, Lund, Sweden
- 80 Nagasaki Institute of Applied Science, Nagasaki, Japan
- 81 Nara Women’s University (NWU), Nara, Japan
- 82 National and Kapodistrian University of Athens, School of Science, Department of Physics , Athens, Greece
- 83 National Centre for Nuclear Research, Warsaw, Poland
- 84 National Institute of Science Education and Research, Homi Bhabha National Institute, Jatni, India
- 85 National Nuclear Research Center, Baku, Azerbaijan
- 86 National Research Centre Kurchatov Institute, Moscow, Russia
- 87 Niels Bohr Institute, University of Copenhagen, Copenhagen, Denmark
- 88 Nikhef, National institute for subatomic physics, Amsterdam, Netherlands
- 89 NRC Kurchatov Institute IHEP, Protvino, Russia
- 90 NRC ÁŃKurchatov InstituteÁŃ - ITEP, Moscow, Russia
- 91 NRNU Moscow Engineering Physics Institute, Moscow, Russia
- 92 Nuclear Physics Group, STFC Daresbury Laboratory, Daresbury, United Kingdom
- 93 Nuclear Physics Institute of the Czech Academy of Sciences, Řež u Prahy, Czech Republic
- 94 Oak Ridge National Laboratory, Oak Ridge, Tennessee, United States
- 95 Ohio State University, Columbus, Ohio, United States
- 96 Petersburg Nuclear Physics Institute, Gatchina, Russia
- 97 Physics department, Faculty of science, University of Zagreb, Zagreb, Croatia
- 98 Physics Department, Panjab University, Chandigarh, India
- 99 Physics Department, University of Jammu, Jammu, India
- 100 Physics Department, University of Rajasthan, Jaipur, India
- 101 Physikalisches Institut, Eberhard-Karls-Universität Tübingen, Tübingen, Germany
- 102 Physikalisches Institut, Ruprecht-Karls-Universität Heidelberg, Heidelberg, Germany
- 103 Physik Department, Technische Universität München, Munich, Germany
- 104 Politecnico di Bari, Bari, Italy
- 105 Research Division and ExtreMe Matter Institute EMMI, GSI Helmholtzzentrum für Schwerionenforschung GmbH, Darmstadt, Germany
- 106 Rudjer Bošković Institute, Zagreb, Croatia
- 107 Russian Federal Nuclear Center (VNIIEF), Sarov, Russia

- 108 Saha Institute of Nuclear Physics, Homi Bhabha National Institute, Kolkata, India
- 109 School of Physics and Astronomy, University of Birmingham, Birmingham, United Kingdom
- 110 Sección Física, Departamento de Ciencias, Pontificia Universidad Católica del Perú, Lima, Peru
- 111 Shanghai Institute of Applied Physics, Shanghai, China
- 112 St. Petersburg State University, St. Petersburg, Russia
- 113 Stefan Meyer Institut für Subatomare Physik (SMI), Vienna, Austria
- 114 SUBATECH, IMT Atlantique, Université de Nantes, CNRS-IN2P3, Nantes, France
- 115 Suranaree University of Technology, Nakhon Ratchasima, Thailand
- 116 Technical University of Košice, Košice, Slovakia
- 117 Technische Universität München, Excellence Cluster 'Universe', Munich, Germany
- 118 The Henryk Niewodniczanski Institute of Nuclear Physics, Polish Academy of Sciences, Cracow, Poland
- 119 The University of Texas at Austin, Austin, Texas, United States
- 120 Universidad Autónoma de Sinaloa, Culiacán, Mexico
- 121 Universidade de São Paulo (USP), São Paulo, Brazil
- 122 Universidade Estadual de Campinas (UNICAMP), Campinas, Brazil
- 123 Universidade Federal do ABC, Santo Andre, Brazil
- 124 University of Cape Town, Cape Town, South Africa
- 125 University of Houston, Houston, Texas, United States
- 126 University of Jyväskylä, Jyväskylä, Finland
- 127 University of Liverpool, Liverpool, United Kingdom
- 128 University of Science and Technology of China, Hefei, China
- 129 University of South-Eastern Norway, Tonsberg, Norway
- 130 University of Tennessee, Knoxville, Tennessee, United States
- 131 University of the Witwatersrand, Johannesburg, South Africa
- 132 University of Tokyo, Tokyo, Japan
- 133 University of Tsukuba, Tsukuba, Japan
- 134 Université Clermont Auvergne, CNRS/IN2P3, LPC, Clermont-Ferrand, France
- 135 Université de Lyon, Université Lyon 1, CNRS/IN2P3, IPN-Lyon, Villeurbanne, Lyon, France
- 136 Université de Strasbourg, CNRS, IPHC UMR 7178, F-67000 Strasbourg, France, Strasbourg, France
- 137 Université Paris-Saclay Centre d'Etudes de Saclay (CEA), IRFU, Département de Physique Nucléaire (DPhN), Saclay, France
- 138 Università degli Studi di Foggia, Foggia, Italy
- 139 Università degli Studi di Pavia, Pavia, Italy
- 140 Università di Brescia, Brescia, Italy
- 141 Variable Energy Cyclotron Centre, Homi Bhabha National Institute, Kolkata, India
- 142 Warsaw University of Technology, Warsaw, Poland
- 143 Wayne State University, Detroit, Michigan, United States
- 144 Westfälische Wilhelms-Universität Münster, Institut für Kernphysik, Münster, Germany
- 145 Wigner Research Centre for Physics, Hungarian Academy of Sciences, Budapest, Hungary
- 146 Yale University, New Haven, Connecticut, United States
- 147 Yonsei University, Seoul, Republic of Korea